

# Online Research @ Cardiff

This is an Open Access document downloaded from ORCA, Cardiff University's institutional repository: <https://orca.cardiff.ac.uk/id/eprint/107693/>

This is the author's version of a work that was submitted to / accepted for publication.

Citation for final published version:

Al-Farraj, Abbas, Marsh, Richard ORCID: <https://orcid.org/0000-0003-2110-5744>, Steer, Julian ORCID: <https://orcid.org/0000-0002-3003-4768> and Valera Medina, Agustin ORCID: <https://orcid.org/0000-0003-1580-7133> 2019.  
Kinetics and performance of raw and torrefied biomass in a continuous bubbling fluidized bed gasifier. Waste and Biomass Valorization 10 (5) , pp. 1365-1381. 10.1007/s12649-017-0167-8 file

Publishers page: <https://doi.org/10.1007/s12649-017-0167-8>  
<<https://doi.org/10.1007/s12649-017-0167-8>>

Please note:

Changes made as a result of publishing processes such as copy-editing, formatting and page numbers may not be reflected in this version. For the definitive version of this publication, please refer to the published source. You are advised to consult the publisher's version if you wish to cite this paper.

This version is being made available in accordance with publisher policies.

See

<http://orca.cf.ac.uk/policies.html> for usage policies. Copyright and moral rights for publications made available in ORCA are retained by the copyright holders.





# Kinetics and Performance of Raw and Torrefied Biomass in a Continuous Bubbling Fluidized Bed Gasifier

A. Al-Farraj<sup>1,2</sup> · R. Marsh<sup>1</sup> · J. Steer<sup>1</sup> · A. Valera-Medina<sup>1</sup>

Received: 19 June 2017 / Accepted: 9 December 2017 / Published online: 16 December 2017  
© The Author(s) 2017. This article is an open access publication

## Abstract

This paper is an experimental study of the kinetics of gasification of olive kernel by using a thermogravimetric fluidized bed reactor technique. Gasification of ‘as received’ and torrefied olive kernels were investigated in a lab-scale bubbling fluidized bed gasifier, operating at up to 3.2 kg/h. The effect of bed temperature between 550 and 750 °C in 50 °C increments on the gasification product gas at mass-based equivalence ratios of 0.15 and 0.2 was studied. To explore the potential of torrefied biomass, the gasification results were compared to that of the ‘as received’ biomass. The product gas from torrefied biomass produced higher H<sub>2</sub>, CO and CH<sub>4</sub> concentrations at identical oxidant flow rates in addition to higher cold gas efficiency and higher product gas heating value. The influence of equivalence ratio in gasification was also investigated at reactor temperatures of 750 °C and five equivalence ratios (0.15, 0.2, 0.25, 0.3, and 0.35). The results revealed that the torrefied biomass has the highest HHV at an equivalence ratio of 0.2 with a value of 6.09 MJ/Nm<sup>3</sup>, while ‘as received’ biomass 4.72 MJ/Nm<sup>3</sup>. Kinetic experiments under isothermal conditions were performed for the gasification of the materials in continuous mode. A mass balance model was successfully used to provide the capability of separately determining the rate constant of the reactions taking place. The kinetic parameters were calculated by a first order reaction model giving activation energies for ‘as received’ olive kernels of 84 kJ/mol and for torrefied olive kernels of 106 kJ/mol.

**Keywords** Gasification · Olive kernel · Torrefied · Biomass · Bubble fluidized bed · Kinetics · Mass balance model

## Introduction

Gasification is an oxidizing process that converts a solid fuel into an energy-rich gaseous product, and it is accomplished by providing less than the stoichiometric oxygen requirement for complete combustion. It is an intermediate stage between combustion and pyrolysis, occurring at temperatures ranging between 600 and 1500 °C [1]. Gasification is considered a viable route by which solid biofuel can be converted partially into gases [2]. Product gas quality is influenced by composition and energy content, which depends mainly upon factors including gasifier configuration, feedstock origin and operating conditions such as equivalence ratio (ER) and temperature [3].

Biomass can be processed into a refined solid biofuel through torrefaction, whose characteristics are intermediate between biomass and coal [4]. The torrefaction process is a mild thermal pre-treatment that is carried out in an inert environment at a temperature between 200 and 300 °C. Under these conditions, the biomass properties are altered through limited devolatilization. Lower moisture, higher energy density, improved ignitability, reactivity and grindability are the characteristics of torrefied biomass when compared to its parent (as received) biomass. However there still remains inadequate information on the gasification performance of torrefied biomass over a range of gasification temperatures. Furthermore, limited published data concerning gasification of torrefied biomass and its impact on syngas composition have been published so far [5]. In addition to this the gasification kinetics of torrefied biomass under continuous operation has not been investigated, since kinetics research has focussed on single-batch tests. Fluidized bed gasification of biomass has the ability of being scaled-up to medium and large scales, overcoming the limitation found in fixed bed designs [6]. In addition to this, fluidized beds

✉ A. Al-Farraj  
Al-FarrajAA@cardiff.ac.uk

<sup>1</sup> School of Engineering, Cardiff University, Cardiff, UK

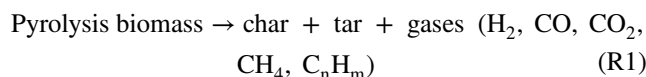
<sup>2</sup> Chemical Engineering Department, AL-Nahrain University, Baghdad, Iraq

provide approximately isothermal conditions with the sand bed and a high heat transfer rate to the reacting fuel mass [7].

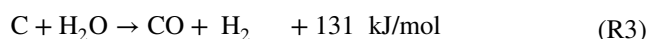
Kinetic research is crucial in understanding the thermochemical processes in gasification. The determination of the kinetics of gasification is essential for modelling the gasification process and extrapolating this to an industrial scale and performance optimisation [8], because the gasification rate is not only influenced by a number of process variables, such as temperature and composition of reactant material, but also by the physical effects such as reactant diffusion and heat transfer. The gasification performance mainly depends on the gasification parameters such as ER, temperature, and the reactivity of a particular sample. For example, the rate of diffusion of material (reactant) may play an important role in the behaviour of reaction. Thus, the successful design of a gasifier, as well as its modelling, requires reliable kinetic data [9]. Fundamental to the combustion or gasification rate are the rates of pyrolysis and char oxidation. The standard method of measuring these rates is via thermogravimetric analysis (TGA) under inert and oxidizing conditions, whereby a small sample of the feedstock (5–15 mg typically) is heated at a certain rate while simultaneously recording mass, time and temperature. TGA is used extensively to study the kinetic parameters of gasification of biomass with CO<sub>2</sub> as a function of mass loss [9–11]. TGA can be considered to be a fixed reactor technique with a relatively low heating rate compared to larger scale systems where biomass is added directly to the reactor at the reaction temperature so the particle heating rate is significantly greater. Meanwhile, the chemical processes in TGA are affected by the interfacial gas diffusion between the reactor space and the solid sample inside the TGA cell [12]. According to Miura and Silveston [13], TGA is suitable for the measurement of slow reaction rates in stable materials. Therefore, there is scientific value in developing apparatus for the kinetic study of biomass gasification that has the same principle of measurement, but utilises a fluidized bed, operating under a high heating rate with a continuous biomass feed.

The thermogravimetric fluidized bed reactor (TGFBR) designed and developed in previous work has been applied to studying the kinetics of biomass gasification with continuous feeding [14]. The design idea of the TGFBR was: (1) to take account of heat and mass transfer using a fluidized bed, (2) providing a rapid heating rate compared to conventional TGA, (3) real time dynamic measurement of biomass conversion. This paper deals with the study of gasification kinetics of as received olive kernels (AROK) and as received torrefied olive kernels (ARTOK) at atmospheric pressure under a continuous feeding rate. The purpose of this study is to explore the kinetics of biomass gasification (raw and torrefied) in a bubbling fluidized bed gasifier. The gasification performance of raw and torrefied biomass are compared across a range of temperatures and ERs.

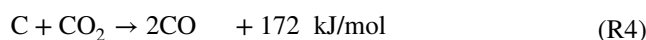
The product gas composition in the gasifier was the result of the combination of a series of competing reactions, as given in reactions (R1)–(R10). Bed temperature is one of the most significant parameters affecting all the chemical reactions included in the combustion and gasification process. In order to simplify the gasification mechanism, the proposed reaction scheme was used to explain biomass gasification in the fluidized bed as follows [15, 16]:



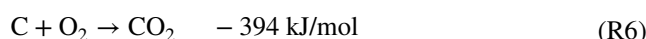
#### Water gas



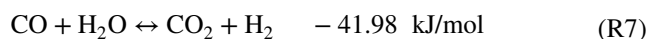
#### Boudouard



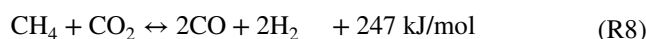
#### Oxidation reaction



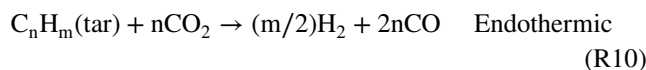
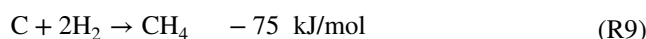
#### Water gas shift reaction



#### Dry reforming



#### Methanation reaction



## Materials and Methods

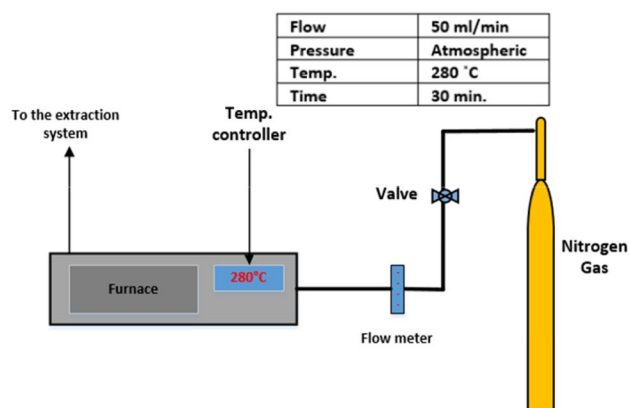
### Olive Kernel Biomass

Olive kernel biomass, a widely available agro-industrial residue of Mediterranean origin, were received as coarse particles with an approximate size of less than 5 mm. The initial moisture content of the olive kernel was measured as 13.3%. The samples were dried to 5.3% moisture content and stored in sealed sacks.

According to ISO DIS 18134 (14774-3) (moisture content), BS EN ISO 15148:2009: (volatile matter content) and BS EN 14775:2009 (ash content) the proximate analysis was determined. Fixed carbon (FC) is defined as the solid residue left after determination of the above, and hence was calculated 'by difference'. The high heating value of biomass was measured using a Parr 6100 bomb calorimeter. Table 1 illustrates the proximate and ultimate analysis (determined

**Table 1** Higher heating values, proximate and ultimate analysis of AROK and ARTOK

Proximate analysis (wt%, wet basis)			
AROK		ARTOK	
Fixed carbon	18.0	Fixed carbon	26.8
Volatile matter	76.0	Volatile matter	68.9
Ash	0.7	Ash	2.0
Moisture	5.3	Moisture	2.2
HHV(MJ kg <sup>-1</sup> )	19.20	HHV (MJ kg <sup>-1</sup> )	20.8
Ultimate analysis (wt%, dry basis)			
AROK		ARTOK	
C	50.93	C	56.93
H	6.16	H	6.32
N	0.01	N	0.14
S	0.02	S	0.02
O	42.11	O	35.66
Ash	0.77	Ash	0.93

**Fig. 1** Schematic setup of the bench torrefaction unit

using a Vario cube Elemental Analyser) of biomass and higher heating values.

## Torrefaction Experiments

A lab-scale Carbolite furnace and nitrogen supply was used to torrefy the olive kernel samples. A batch of 50 g of AROK sample was loaded into a steel tray, and inserted into the furnace at pre-set temperature of 280 °C and 30-min residence time under a nitrogen flow. The nitrogen flow was used to keep the system inert by eliminating the presence of oxygen and to sweep volatile products from the furnace. The torrefaction temperature and residence time of 30 min were selected to be optimal for torrefaction experiment from preliminary studies [17, 18]. Figure 1 illustrates a schematic view of the experimental setup.

Two of the most important parameters in evaluating torrefaction are the mass and energy yield of the process. The mass and energy yields of the biomass were calculated, based on equations cited by Poudel et al. [19] as:

$$\text{Mass yield } (Y_{\text{mass}}) = \left( \frac{\text{Mass after torrefaction}}{\text{Mass of raw sample}} \right) \times 100 \% \quad (1)$$

$$\text{Energy yield } (Y_{\text{energy}}) = Y_{\text{mass}} \left( \frac{\text{HHV}_{\text{torrefied sample}}}{\text{HHV}_{\text{raw sample}}} \right) \times 100 \% \quad (2)$$

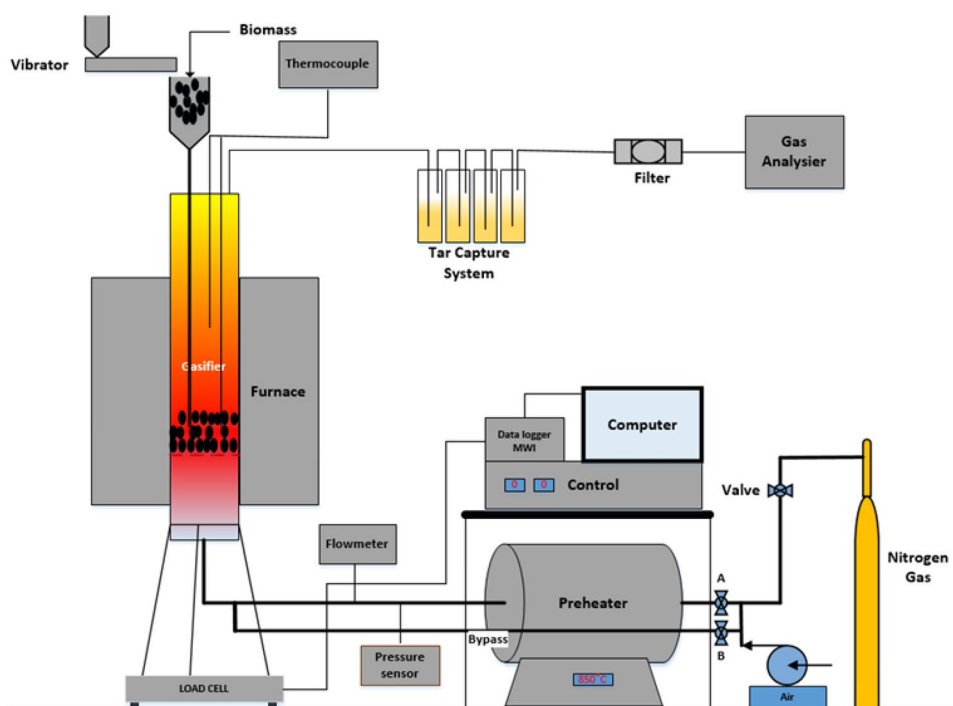
## Experimental Setup of Fluidized Bed

A pilot scale TGFBR, designed and fabricated in the School of Engineering at Cardiff University was used in this study. A schematic diagram of the TGFBR is illustrated in Fig. 2. The system essentially consists of six parts: biomass feeding system, gasifier (which consists of an air box section and perforated distributor plate), air delivery system, heating system, downstream gas cleaning, and product gas analysis.

The vertical stainless-steel reactor was 83 mm i.d. and 1250 mm tall. A perforated diffuser plate was made from stainless steel of 5 mm thickness and uniformly perforated with 151 holes of 1 mm diameter in a triangular pitch; this plate was used to retain the bed fluidization material. A perforated plate was used in this study because it improved the mixing significantly (less segregation tendency) compared to a porous plate [20]. The fluidizer was surrounded by a split tube furnace (3-zone) with maximum set point temperature of 1200 °C. The fluidizing nitrogen was preheated by passing it through a 50 mm i.d. 670 mm long tube containing impervious alumina porcelain (IAP) as a heat transfer medium. The tube was surrounded by electrical preheater



**Fig. 2** Schematic of thermo-gravimetric fluidised bed reactor



supplied by Linton tube furnaces. The preheater can adjust the outlet gas up to 650 °C.

The fluidized bed sat on a bespoke platform load cell designed and built for this experiment by Coventry Scale Company. The balance has a tolerance of  $\pm 0.5$  g and a weighing range up to 25 kg. A multifunction weight indicator model DFW06XP was connected to a load cell and through a computer used to record the mass change continuously at 1 s time intervals.

In order to monitor the temperature of the reactor, two Type-K thermocouples were positioned in the reactor at the location marked in Fig. 2. One of the thermocouples was installed in the bed zone (30 mm above the distributor plate) and the other was located in the freeboard (350 mm above the distributor plate). Data acquisition hardware (from Omega) was connected to the computer to continuously record the temperatures in the bed and freeboard. DAQ central data logging software was installed in the host computer. A high-speed USB cable transferred the data from the Multiple Channel Data Acquisition Module, model number (OMDAQ-USB-2401) to the computer. When data acquisition was complete, the data was exported to Excel for analysis.

## Experimental Procedure

### Gasification Procedure

The minimum fluidization velocity  $U_{mf}$  was determined prior to the gasification tests in previous studies and was found equal to 20 l/min (0.06 m/s) for 500–600  $\mu$ m diameter silica

sand at elevated temperature [14]. The superficial velocity used in this study was  $2U_{mf}$  (0.12 m/s). For a particle to be carried out of the bed, the local gas velocity needs to exceed the particle's terminal velocity, which is the speed at which an object in free fall is no longer accelerating [21]. Therefore, one aim of this study was to keep the superficial velocity lower than the terminal velocity to avoid elutriation loss of bed material during experimental work. The terminal velocity was calculated according to Kunni and Levenspiel's equations and found equal to 0.89 m/s, which is above the superficial velocity of the gas (0.12 m/s) [22].

The ER was changed (0.15, 0.2, 0.25, 0.3 and 0.35) by varying the biomass feed rate from 1.38 to 3.24 kg/h for AROK and 1.14 to 2.7 kg/h for ARTOK. The biomass samples were tested at temperatures of 550, 600, 650, 700, 750 °C and at an ER of 0.15 and 0.2. The main operation conditions are summarized in Table 2.

At the start-up of each experiment, the required amount of silica sand (400 g) [this being dependant on the static bed height to bed diameter ratio ( $H_s/D$ ) of 0.5] was added as bed material to the gasifier. It is important to keep the weight measurement away from the vibration effect of fluidization. Therefore, for kinetic purpose study,  $H_s = 0.5 D$  was used in all experiments, because it gave a negligible vibration effect on measurements. The heaters were set to the temperatures under consideration (550, 600, 650, 700, and 750 °C) and the airflow was activated before biomass feeding commenced. The biomass was fed into the reactor through a pre-calibrated Fritsch vibrating feeder connected at the top of the gasifier and the split furnace was switched off. Valve B was opened and valve

**Table 2** Parameters used in gasification experiments of AROK and ARTOK

ER	0.15	0.2	0.25	0.3	0.35
Biomass flow rate with moisture (kg/h) AROK	3.24	2.46	1.98	1.62	1.38
Biomass flow rate with moisture (kg/h) ARTOK	2.7	2.04	1.62	1.38	1.14
Air flow rate (l/min)	40	40	40	40	40

A closed (see Fig. 2) to provide ambient air to quench the heat generated inside the gasifier during gasification. In order to ensure the consistency of the biomass mass flow rate, a known amount of biomass was filled into the vibrator hopper before the gasification test, and after the test the leftover biomass in the hopper was measured to provide a gravimetric check.

During the gasification test, the rig mass measurements recorded the variation of mass inside the gasifier every second, the gas compositions were recorded online by using gas analyser during the gasification test. When the gasifier cooled down, the bed material was removed from the fluidizer and fresh sand added for next test.

### Product Gas Analysis

The extracted gas sample was scrubbed of particulates and volatile matter using four dreschel bottles filled with isopropanol at  $-10^{\circ}\text{C}$ , then passed through a silica gel trap to avoid slippage of solvent. The product gas was analysed using an Emerson X-Stream analyser. Prior to the gasification test, the gas analyser was zero calibrated on  $\text{N}_2$  and then with a certified span gas mixture. The standard gas mixture used for gas analyser calibration comprised of  $\text{CO}$ ,  $\text{CO}_2$ ,  $\text{H}_2$ , and  $\text{CH}_4$  with 15, 15, 15, and 5% by volume concentration respectively. After calibration, the gas sample from the gasifier was connected to the gas analyser to record the volume concentration of the gasification reactions. When the gasification test was finished, the gas analyser was purged with  $\text{N}_2$  and the same steps given above were repeated for another run.

### Gasification Effectiveness

The effectiveness of the gasification process was evaluated in terms of higher heating value of the dry gas ( $\text{HHV}_g$ ), carbon conversion ( $\mu_c$ ) and cold gas efficiency ( $\eta$ ). The dry gas HHV can be estimated from the gas composition by:

$$\text{HHV}_g = (12.75[\text{H}_2] + 12.63[\text{CO}] + 39.82[\text{CH}_4] + \dots)/100 \quad (3)$$

where the species contents are given in mol%, and their heats of combustion, in  $\text{MJ}/\text{Nm}^3$  [23]. The concentrations of

higher hydrocarbons were not measured since an analyser of sufficient accuracy under these conditions was not available.

The biomass was shown to contain only 0.01% nitrogen, so it was considered reasonable to use nitrogen as the tracer for material balance calculations to calculate the dry gas yield [24].

$$Y = \frac{Q_a \times 79\%}{W_c N_2\%} \quad (4)$$

where  $Q_a$  is the volume flow rate of air ( $\text{Nm}^3/\text{h}$ ),  $W_c$  is the biomass mass flow rate ( $\text{kg}/\text{h}$ ), and  $N_2\%$  is the volumetric percentage of  $\text{N}_2$  in the dry fuel gas.

The carbon conversion efficiency to product gas was determined on the basis of the gas analysis (volumetric percentage of the fuel gas composition of  $\text{CO}$ ,  $\text{CO}_2$ , and  $\text{CH}_4$ ) as follows:

$$\mu_c = \frac{Y(\text{CO}\% + \text{CO}_2\% + \text{CH}_4\%) \times 12}{22.4 \times C\%} \times 100\% \quad (5)$$

where  $C\%$  is the mass percentage of carbon in the ultimate analysis of biomass as shown in Table 1.

The cold gas efficiency is used to account for the performance of biomass gasification. It is defined as the ratio of chemical energy in the gas to that in the fuel [25]. This definition excludes the heating value of the condensable substances such as tars, therefore cold gas efficiency is the percentage of the fuel heating value converted into the heating value of the product gas.

The cold gas efficiency was given by:

$$\eta = \frac{\text{HHV}_g \times Y}{\text{HHV}_f} \times 100\% \quad (6)$$

where  $\text{HHV}_g$  is the higher heating value of the product gas in  $\text{MJ}/\text{Nm}^3$ ,  $\text{HHV}_f$  denotes the gross calorific value of the fuel in  $\text{MJ}/\text{kg}$ .

### Char Yield of Pyrolytic Biomass

Char yield,  $Y_{ch}$ , refers to the char remaining after devolatilization of biomass. Bio-char can be obtained from biomass pyrolysis [26]. The char obtained from the gravimetric method is closely analogous to the actual conditions in a fluidized bed gasifier, because no cooling occurred between the devolatilization stage and gasification [27]. Therefore, this procedure was used to investigate the char yield of biomass under inert conditions (nitrogen gas) by using a similar superficial velocity to that of a full-scale industrial system. Both AROK and ARTOK were tested under 40 l/min  $\text{N}_2$  at a temperature of 525 and 550  $^{\circ}\text{C}$  under the assumption that the char yield remains approximately the same, and to maintain consistency of calculations.

Zabaniotou et al. [28] reported that the olive kernel char yield decreased with increasing temperature during pyrolysis up to 500 °C after that the yield tends to be constant. According to Blasi, the final char yield is less affected when the temperature is increased above 650–750 K (377–477 °C) for all particle sizes. Consequently, even though for different reasons, for both pyrolysis regimes, the char yield tends to a constant value as the temperature is increased [29]. It is necessary to calculate char yield during pyrolysis conditions to determine kinetics later in the gasification experiments.

## Kinetic Modelling Approach

A transient mass balance model as derived and evaluated by Timmer [30] was used to predict the mass of the carbon in the reactor at any time 't'. However, the rate constant of this model was estimated by assumption that the steady state condition was achieved and the amount of carbon accumulated is also estimated by stopping feeding of biomass and observing the rate of combustion in the reactor, since the system will subsequently become air rich and hence the remaining carbon can be quantified via mass balance of the produced CO<sub>2</sub>. In this study, the same mass balance model was used for char to determine the rate constant of biomass reaction in a continuous gasification process depending on real steady state conditions inside the gasifier and continuous monitoring of char build up inside the reactor, neglecting solid particle elutriation [31].

Char conversion is a key factor governing the effectiveness of fluidized bed gasification [27]. This method utilises a mass balance of the char as it enters and reacts in the gasifier. According to the same author, Eq. (7) was used describe char conversion of biomass under fluidized bed gasification.

$$F = m_f^0 Y_{ch} \quad (7)$$

where F is char feed rate in g/s,  $Y_{ch}$  is the char yield after devolatilization (mass of char per mass of biomass),  $m_f^0$  is biomass feed rate (g/s).

The differential change in the mass of char solid particles ( $dm$ ) in the gasifier during time ( $dt$ ) was as follows:

$$dm = Fdt - R_r dt \quad (8)$$

where  $R_r$  is chemical reaction rate of char in g/s.

For a first-order reaction of biomass [32–36]

$$R_r = km \quad (9)$$

where k is the rate constant ( $s^{-1}$ ) and m is mass of char solid particles in the reactor. By substituting Eq. (9) into (8):

$$\frac{dm}{dt} = F - km \quad (10)$$

Separation of variables yields:

$$\frac{dm}{F - km} = dt \quad (11)$$

Given the initial condition,  $m_{(t=0)} = 0$ , Eq. (11) was integrated and Eq. (12) was obtained.

$$m(t) = \frac{F}{k} [1 - \exp(-kt)] \quad (12)$$

where  $m(t)$  is the mass of char at any time t.

According to Timmer, given sufficient time under consistent gasification conditions the mass of solid in the reactor approaches steady state, hence Eq. (12) reduces to:

$$m_{ss} = \frac{F}{k} \quad (13)$$

Equation (13) allows calculation of k if F and  $m_{ss}$  are known. In this study, a steady state  $m_{ss}$  was measured experimentally and the rate constant was evaluated at five different temperatures.

The value of k was inserted into Eq. (12) to evaluate theoretically the amount of char with time during the gasification. The theoretical and experimental work were then compared. To evaluate the degree of fit of the predicted values versus the experimental values, this study used the coefficient of determination (also known as  $R^2$ ) function as follows:

$$R^2 = 1 - \frac{\sum_{i=1}^n (Y_i - \hat{Y}_i)^2}{\sum_{i=1}^n (Y_i - \bar{Y})^2} \quad (14)$$

where Y represents the measured char in the reactor,  $\hat{Y}$  is the corresponding value of the char predicted by the model, n is the total number of data, and  $\bar{Y}$  is the mean of the measured char inside the reactor during the gasification run.

Chemical rate controlled reactions tend to increase with temperature typically following the Arrhenius Equation (15), where  $E_a$  is the activation energy, A is the pre-exponential factor and R is the universal gas constant.

$$k = A \exp \left[ \frac{-E_a}{RT} \right] \quad (15)$$

## Results

### Fuel Characterization

Data from the proximate analysis and ultimate analysis of AROK and ARTOK are given in Table 1. From the ultimate analysis reported, it can be seen that the oxygen content decreased from 42.11% for AROK down to 35.66% for the torrefied (ARTOK) biomass. In terms of the O/C ratio, the value decreased from 0.82 for AROK down to 0.62 for the ARTOK; which is in agreement with literature [37] and the

mass and energy yield were 86 and 93% respectively (where energy yield represents the ratio of actual energy conserved after the torrefaction process to the initial energy content of biomass). A typical mass and energy yield of woody biomass torrefaction is that 70% of the mass is retained as a solid product, containing 90% of the initial energy content [4, 38]. These results agreed with Prins et al. [39], who found that during parent biomass torrefaction, the volatile matter decreased from ca. 80 to 60–75%, while the heating value increases by 5–25%.

### Gasifier Operation

Figure 3 shows the recorded reactor temperatures during the gasification experiments at reactor preset temperatures of 550, 600, 650, 700, and 750 °C for AROK and ARTOK. Time  $t=0$  symbolises the start of biomass feeding into the reactor. As each result shows, the process initially undergoes a heating phase, where the thermochemistry within the reactor is approaching equilibrium, generally considered to be endothermic. When the heat generation rate matches or exceeds the rate of heat loss, the process becomes thermochemically self-sustaining [40]. The middle portion of the figure represents the gasification reaction phase, and it is clear that the initially unstable process has reached thermal equilibrium. This resultant temperature is used in the calculation of the reaction kinetics. Comparing the biomass samples, the ARTOK generally reached steady-state conditions at higher temperatures than the AROK at identical preset temperatures. This is in agreement with other work [41], where the same phenomena during the gasification of raw and torrefied biomass was observed. According to Bridgeman et al., there is possible explanation for this phenomenon as follows. During gasification, the initial volatiles released from AROK are low in calorific value being principally composed of water and carbon dioxide, and that any

combustible gases are not particularly energetic. Therefore, the energy required to release the water and carbon dioxide is compensated by the energy produced from combustion of the low energy volatiles, leading to marginal, if any, energy gain. When the biomass has been torrefied, the energy intensive water and carbon dioxide has been lost, as have any low energy volatiles. Therefore, when ARTOK is gasified, higher temperatures are achieved, as in Fig. 7a, b, because it contains high energy volatiles and char which react directly to produce higher temperatures [37].

Biomass feeding was halted when the mass variation in the experiment was less than 1 g per second, with the air flow maintained constant. The data in Fig. 3 show that the response to the stop in feeding was a rapid temperature increase (commencing within 5 s after the feeder stopped). This is attributed to the reactor stoichiometry shifting into the combustion regime, thus providing more exothermic conditions as the remaining mass of biomass in the bed is oxidised under excess air.

### Effect of Bed Reactor Temperature on the Gas Yield

Figures 4 and 5 show the product gas composition ( $\text{CO}$ ,  $\text{CO}_2$ ) and ( $\text{H}_2$ ,  $\text{CH}_4$ ) as a function of the gasifier temperature of AROK and ARTOK at  $\text{ER}=0.15$  and  $\text{ER}=0.2$ . The major gasification reactions R2, R3 and R4 are endothermic processes while the methanation reaction R9 is exothermic. It is known that the water gas and Boudouard reactions (R3 and R4) are favoured at higher temperature [40]. Water vapour and  $\text{CO}_2$  promote  $\text{H}_2$  production in the biomass gasification process [42]. The influence of bed temperature on these reactions likely explains the findings where, as bed temperature was increased, the concentration of  $\text{CO}$  and  $\text{H}_2$  increased while the concentration of  $\text{CO}_2$  decreased.  $\text{CH}_4$  was produced at comparatively low concentrations (< 7 vol%) under all test conditions. At atmospheric pressure,  $\text{CH}_4$  from the

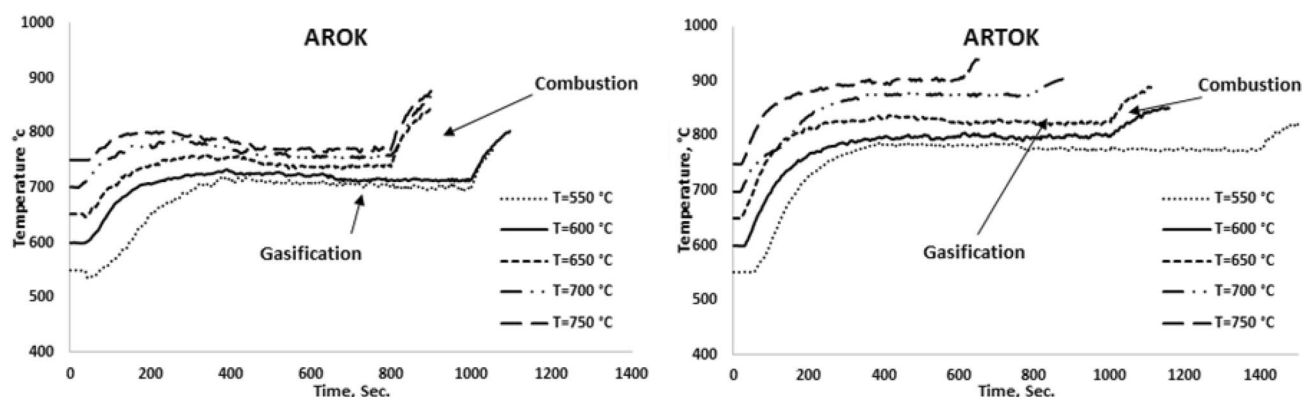


**Fig. 3** Stable temperature zone in the gasifier for gasification of AROK and ARTOK, including the initiation point of combustion just after the biomass feed was stopped



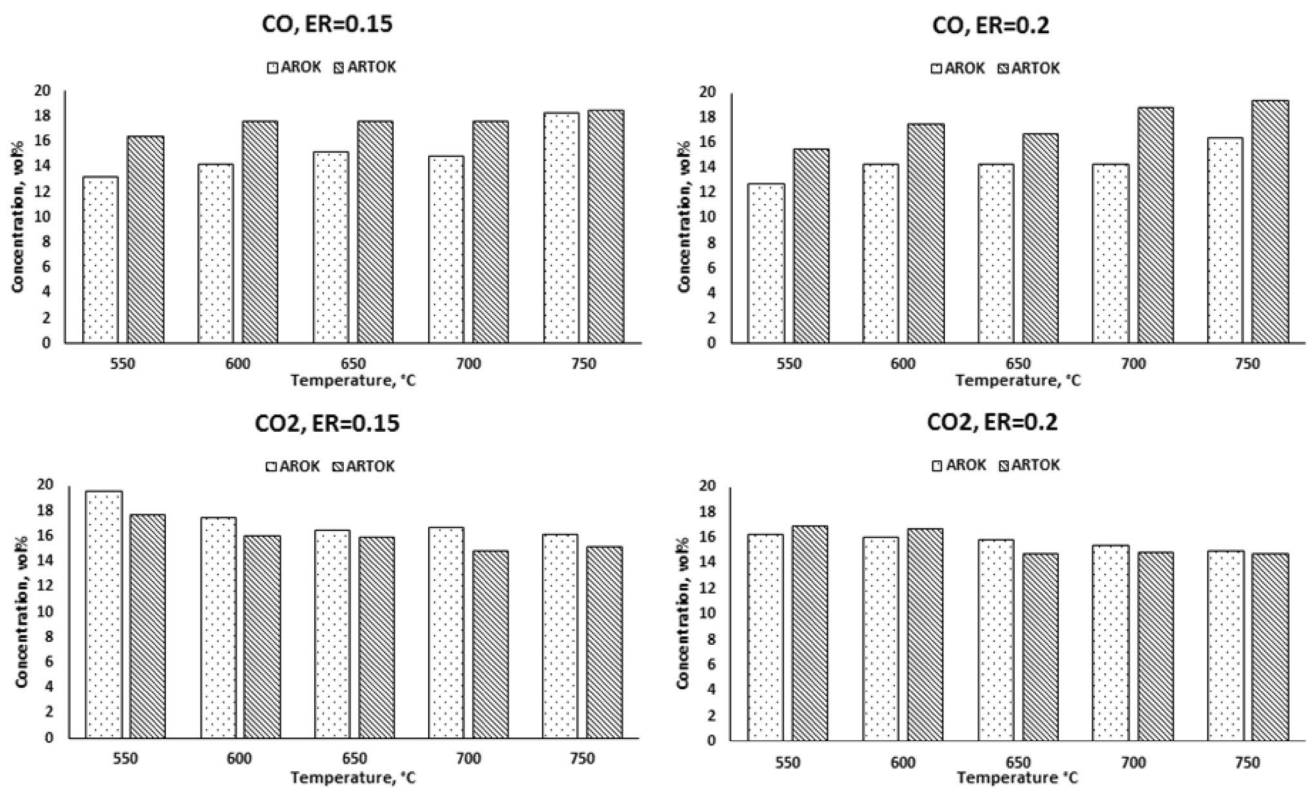


Fig. 4 Comparison of CO and CO<sub>2</sub> gas in as received torrefied olive kernels at ER=0.15, 0.2 and different bed temperatures

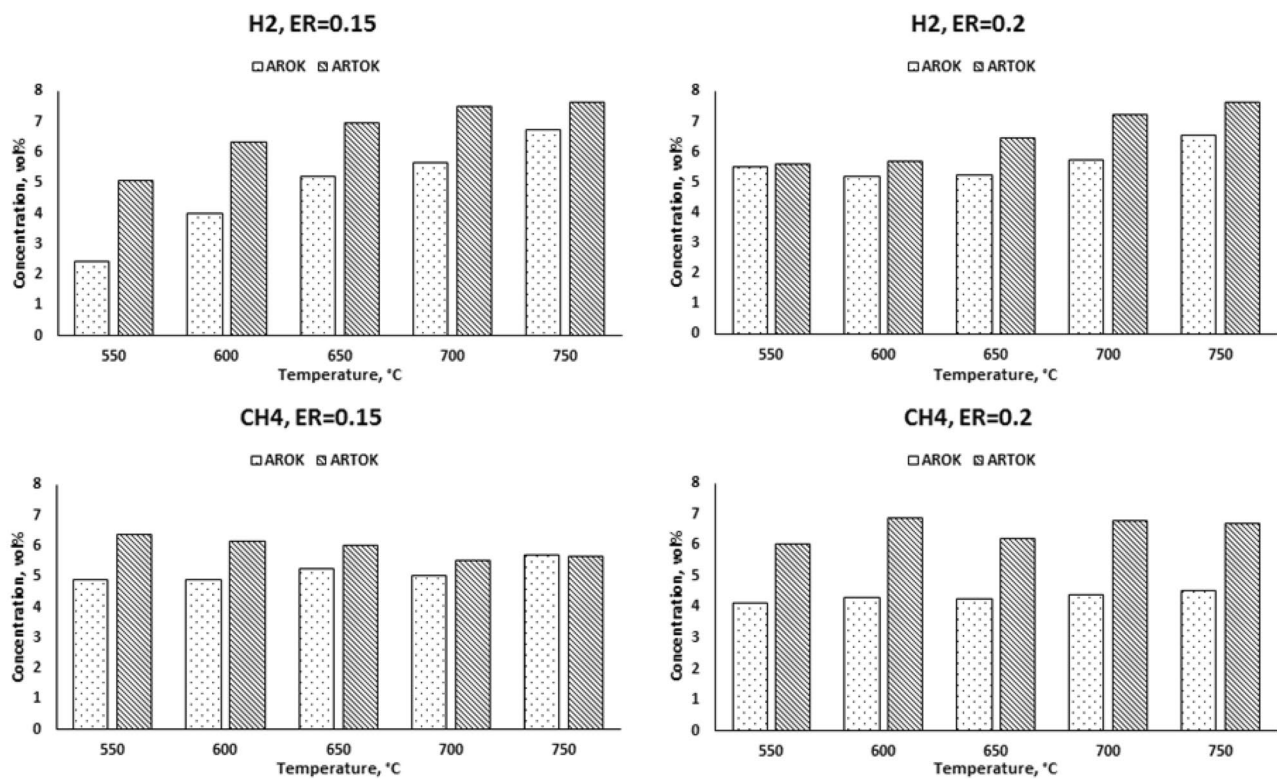


Fig. 5 Comparison of H<sub>2</sub> and CH<sub>4</sub> in as received and as received torrefied olive kernels at ER=0.15, ER=0.2 and different bed temperatures

syngas is normally the product of biomass pyrolysis, i.e. from reaction R1 [16]. At higher temperatures, the gas generated from biomass in the pyrolysis zone could undergo further reactions (secondary reactions) such as tar cracking, as described by reaction R2, which leads to an increase in  $\text{CH}_4$  concentration with bed temperature. Skoulou et al. [43] demonstrated that methane was generally produced at low concentration ( $\text{CH}_4 < 5 \text{ vol}\%$ ) under all test conditions from olive kernels in a fluidized bed reactor and they explained that methane was reforming at higher temperatures due to reaction R2. The same result was obtained by Mohammed et al. [44] and Lucas et al. [45]. The trends of  $\text{CH}_4$  did not show obvious variation with temperature; this could be due to thermal cracking at high temperature as the char methanation reaction rate for reaction R9 is relatively slow compared with other reactions [46], or the generated  $\text{CH}_4$  can be consumed through methane dry reforming via R8. Thus, it seems there was a balance between  $\text{CH}_4$  generated and consumption rate that kept the methane level approximately constant even at high temperature. This trend of methane not showing obvious variation is in agreement with results published by Xue et al. [47] when torrefied *Miscanthus × giganteus* was gasified in an air-blown bubbling fluidized bed gasifier.

The analysis indicates that the gasification of the ARTOK produced more CO and less  $\text{CO}_2$  than the parent AROK with the exception of temperatures below  $650^\circ\text{C}$  at  $\text{ER} = 0.2$ . The oxygen content of ARTOK was lower than that of AROK and the FC content was higher, which enhanced the Boudouard reaction (R4). According to Kuo et al. [48] the gasification of raw biomass gives lower CO concentration than torrefied biomass, which is stemming from the lower carbon content of raw biomass. The marginal behaviour of  $\text{CO}_2$  concentration at  $\text{ER} = 0.2$  is likely due to the water gas shift reaction (R7) being more dominant at this ER [49].

The gasification of AROK and ARTOK at different temperatures indicated that the ARTOK produced more  $\text{H}_2$  as shown in Fig. 5, which implies that the hydrogen-producing

reactions are being favoured at the higher temperatures provided by the ARTOK reactions. This was expected because the gasification of torrefied biomass produced more  $\text{CH}_4$  gas compared to AROK thus promoting R8. The hydrogen conversion into dry gas was higher for torrefied biomass since the gasification of this feedstock results in higher yield of  $\text{CH}_4$  and  $\text{C}_2\text{H}_6$  [50]. This is in an agreement with Taba et al. [51], who stated that the biomass having low contents of volatile matter is more suitable for significant  $\text{H}_2$  production.

### Effect of Equivalence Ratio

In addition to temperature, ER also had a significant controlling effect on the gasification process including syngas composition. The effects of ER were evaluated for product gases for AROK and ARTOK through a set of experiments, performed at  $T = 750^\circ\text{C}$  and varying ER between 0.15 and 0.35 in 0.05 increments. Different ERs were obtained by varying the biomass feeding rate and keeping the air flow rate constant at 40 l/min.

For both biomass samples examined, the ER had a measurable effect on the concentration of product gases. As the ER was increased (by reducing the fuel biomass flow rate) the CO,  $\text{CH}_4$  and  $\text{H}_2$  concentration decreased since less product gas was being produced per second (see Fig. 6). Given that the air flow was constant, higher concentrations of oxygen were therefore available for gas phase oxidation reactions to occur. This explains the visible reduction in CO,  $\text{CH}_4$  and  $\text{H}_2$ , but a small increase in the  $\text{CO}_2$  [46].

This profile of product gases is comparable to other published results for fluidized bed gasifier rigs. In similar findings, the  $\text{H}_2$  and CO concentrations decrease and the  $\text{CO}_2$  content increases slightly with increasing ER during gasification of pine wood in a bubbling fluidized bed [52, 53].

At high ER, the reduced HHV of the product gas as shown in Fig. 7 was obtained due to a lowering of the concentration of energetic (combustible) species. The carbon conversion efficiency ( $\mu_c$ ) increases with increasing ER for

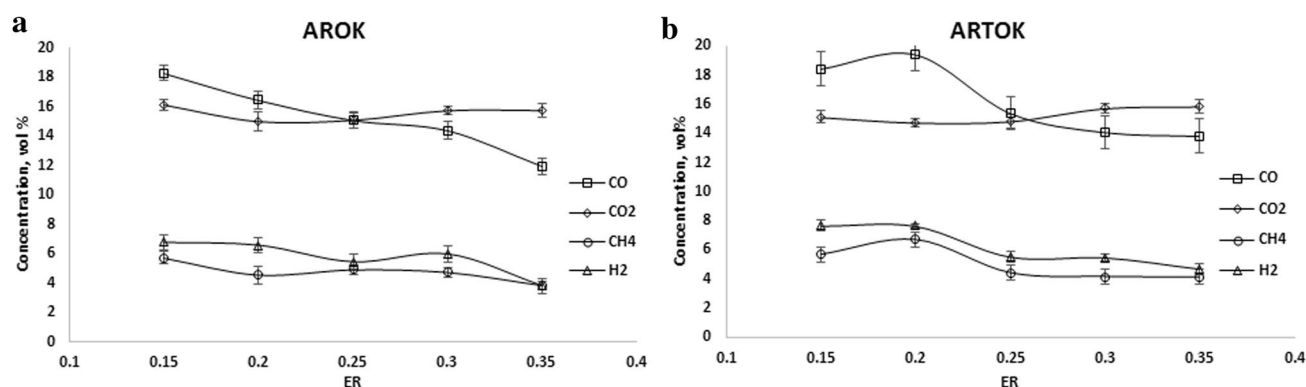


**Fig. 6** Effect of ER (0.15, 0.2, 0.25, 0.3, and 0.35) at  $750^\circ\text{C}$  of **a** AROK and **b** ARTOK on concentration of product gas

both biomass samples, which is attributed to the subsequent gas phase oxidation reactions described above. As a result, the carbon conversion efficiency increases over the range tested for both samples, although this includes conversion into  $\text{CO}_2$ , hence the lowering of HHV. The results obtained agree with an earlier study where biomass was gasified in bubbling fluidized bed [54].

Gas yield is the volume of dry fuel gas generated in  $\text{Nm}^3$  per kg of fuel and is a significant parameter for evaluating the performance of the gasifier. As shown in Fig. 8, for both biomass samples the gas yield increased with increasing ER, but this is coupled with a decrease in HHV, which is logical since the higher concentration of oxygen results in more complete combustion. ARTOK exhibited more gas yield compared to AROK for all ERs tested, which can be accounted for by improved endothermic char gasification reactions [47]. When the gasifier temperatures increase, the carbon conversion increases hence gas yield also increases [51]. The relatively small error bars in the product gas analysis (see Figs. 6, 7, and 8) reflect that the biomass feeder is assumed is reliable, based on calibration tests that were undertaken in the laboratory.

### Effect of Bed Temperature on HHV and Cold Gas Efficiency

The effectiveness of the gasification process was evaluated in terms of HHV of dry gas and cold gas efficiency. Figure 9a and b shows the HHV and  $\eta$  respectively of AROK and ARTOK by varying the bed temperature between 550 and 750 °C in 50 °C increments and using an ER of 0.2.

Figure 9 a illustrates the effect of bed temperature on HHV of the product gas for AROK and ARTOK. An increase of bed temperature from 550 to 750 °C measurably improved the gas HHV from 3.96 to 4.72  $\text{MJ}/\text{Nm}^3$  for AROK and 5.08 to 6.09  $\text{MJ}/\text{Nm}^3$  for ARTOK. As explained earlier, higher temperatures enhanced the evolution of combustible gases

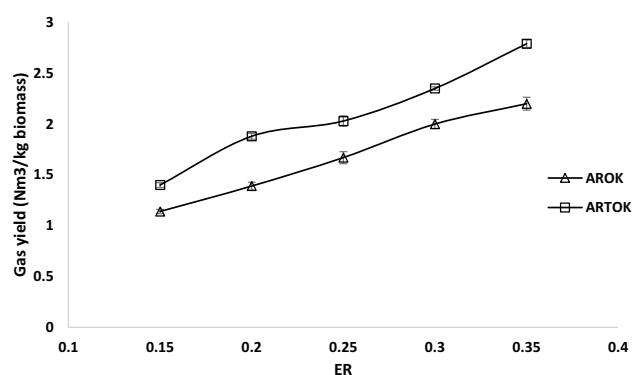


Fig. 8 Influence of ER on gas yield of AROK and ARTOK at 750 °C

especially  $\text{H}_2$  and  $\text{CO}$  which in turn results in an increase in HHV of the product gas.

The variation of cold gas efficiency with temperature is given in Fig. 9b. The highest  $\eta$  values at  $T = 750$  °C of AROK and ARTOK were 34.23 and 55.03% respectively. The higher temperatures contributed to lower concentration of char and heavy tars and led to higher gas yield due to release of more volatiles [55].

External mass transfer resistance is responsible for restricting the flow of volatiles generated in a biomass particle from travelling outward from its surface [56]. From the proximate analysis of the two samples (Table 1) it can be inferred that the external resistance of ARTOK will be less than the AROK. Hence, the volatile matter generated from the AROK will form a comparatively large vapour field around the particles, which displaces oxygen and results in a diffusion-controlled zone around the particle, limiting oxidation reactions with the char. In the case of the ARTOK, the smaller quantity of volatile matter implies that this vapour field is smaller and therefore greater contact with oxygen is permitted, hence a higher reaction rate can be achieved. This is in agreement with Chen et al. [57] who stated that

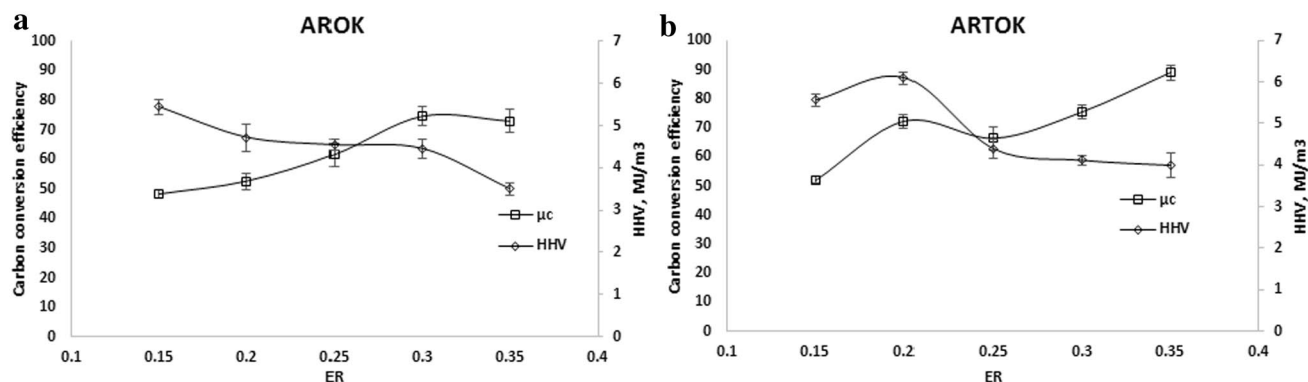
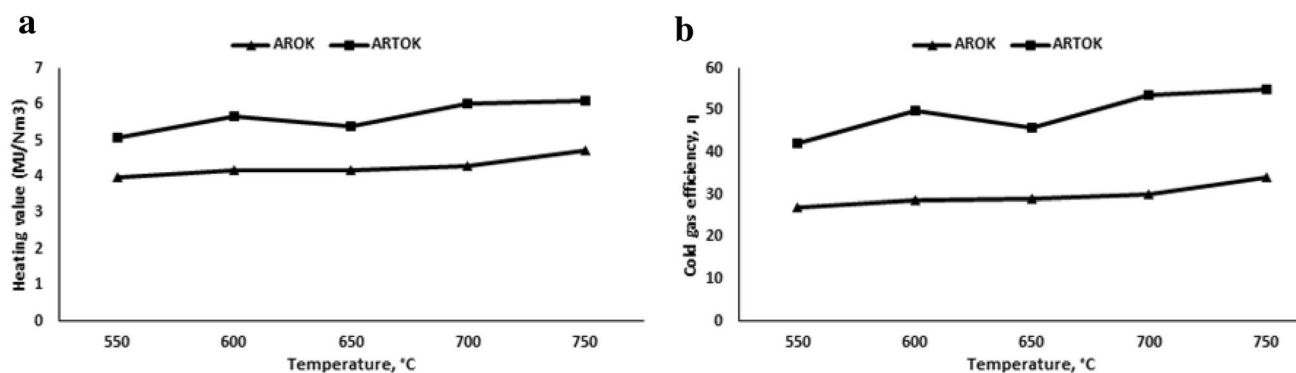


Fig. 7 Effect of ER (0.15, 0.2, 0.25, 0.3, and 0.35) at 750 °C of **a** AROK and **b** ARTOK on carbon conversion efficiency and higher heating value



**Fig. 9** Effect of bed temperature on gasification output performance for AROK and ARTOK **a** HHV and **b**  $\eta$

**Table 3** Rate constant ( $k$ ), steady state temperature and mass load of AROK and ARTOK at the range of steady reaction temperatures examined

AROK (ER=0.2)			ARTOK (ER=0.2)		
Reaction steady temperature (K)	$m_{ss}$ (g)	$k$ ( $s^{-1} \times 10^3$ )	Reaction steady temperature (K)	$m_{ss}$ (g)	$k$ ( $s^{-1} \times 10^3$ )
973	75	1.96	1048	79	1.7
986	59	2.49	1073	49	2.7
1011	49	3	1097	38	3.5
1028	45	3.26	1148	26	5.2
1043	34	4.3	1173	20	6.8

torrefaction improves the physical and chemical characteristics of biomass, hence the syngas quality and cold gas efficiency are improved.

### Influence of Superficial Gas Velocity on Gasification

Maintaining a constant ER between the biomass and air, the superficial gas velocity was altered through the reactor. Increasing the superficial gas velocity will lead to an increase in the degree of agitation and gas-to-particle heat transfer. In the gas–solid reaction, the mass transfer of the gas first takes place from the main stream of fluid to the external surface of the particle [58].

A series of five tests were achieved at temperature 750 °C and ER = 0.2 to investigate the effect of external diffusion on the gasification of AROK and are shown in Fig. 10. This figure gives the calculated mass of instantaneous char remaining inside the gasifier during continuous gasification. The data show that the rate of reaction was affected by changing the superficial velocity up to a velocity of  $2U_{mf}$ , where after the effect appeared to saturate. In this gas–solid reaction system, the mass transfer effects could be minimized when the system is operated at sufficiently high gas velocity, so that the overall reaction rate does not increase with further increase in gas velocity [59]. Therefore, a superficial velocity of  $2U_{mf}$  was selected as the basis for all tests, representing the minimum air

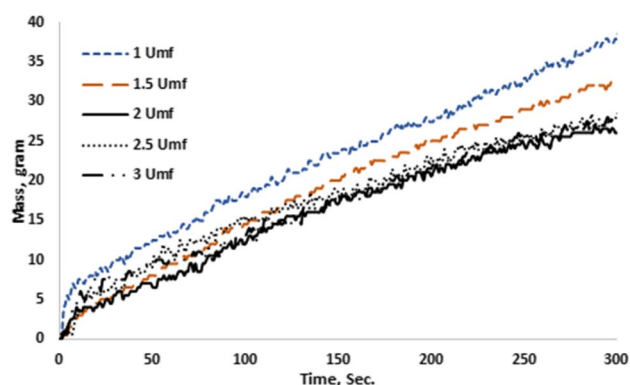


**Fig. 10** Mass of char build up in the gasifier at different superficial velocity at 750 °C and ER=0.2

velocity required to reduce external diffusion. At high gas velocity, the boundary layer thickness around the particle becomes sufficiently small that it no longer offers any resistance to the diffusion of gas, eliminating external diffusion from the reaction rate [60].

### Kinetic Parameters

The controlling kinetic parameters were examined by investigating the mass-time behaviour of the reactor. This was undertaken at five preset temperatures (550, 600, 650,



700, and 750 °C),  $2U_{mf}$  and one ER (0.2) for AROK and ARTOK. All experiments were undertaken at isothermal conditions for a sufficient time until steady state conditions were obtained for each case.

Figure 11 illustrates the instantaneous mass of char in the bed, from initial fuel feeding to steady-state conditions, where there is no further increase in the measured mass of char inside the reactor. The behaviour is shown for both AROK and ARTOK samples, on identical axes scales to aid in comparison. As the system approaches equilibrium during continuous feeding of biomass, the amount of char builds up in the reactor while the rate of devolatilization remains constant. After sufficient time under consistent gasification conditions, steady state char conversion is achieved. As can be seen from the figure, the final equilibrium mass and time are found to be dependent on temperature. The reaction rate is shown to be faster at higher temperatures for both biomass samples [61]. Note that above 550 °C the equilibrium condition mass of ARTOK was always lower than the AROK, since the oxidation of carbon in the char takes place parallel to thermal decomposition and release of volatile matter [62]. Therefore, the equilibrium mass of char at steady state is less for ARTOK. According to Sami et al. [63], the volatiles may burn in jets or as a flame envelope. An enveloping flame acts like a shroud, preventing oxygen from reaching the particle surface and therefore preventing heterogeneous oxidation of char. This is in agreement with Hu et al. who stated that torrefied biomass had a more steady-state burning process and a higher combustion efficiency compared to ‘as received’ biomass [64].

The reduction of the oxygen to carbon ratio in fuels correlates with an increase in resistance to thermal degradation (see the ultimate analysis of AROK and ARTOK), which is one of the objectives of torrefaction and carbonization, justifying the results observed on Fig. 12. It was observed that ARTOK has a lower mass loss rate than AROK due to a higher resistance to thermal degradation. Fuels with higher contents of FC and low volatile matter tend to decompose slowly and offer higher resistance to thermal degradation [65]. This is in agreement with Ren et al. [66] who noticed that the raw biomass lost mass faster than torrefied biomass during the pyrolysis of woody biomass. As shown in Fig. 12, the AROK released volatiles faster during pyrolysis than ARTOK, the time difference being about 2–3 s. Hence, ARTOK has a lower volatile loss rate than AROK, so there is less flow resistance to outward gas diffusion during gasification (see proximate analysis), which gave the ARTOK more opportunity to react with oxygen. Figure 11 shows the mass change of ARTOK, under the temperatures described at ER = 0.2. The data in Fig. 11 therefore demonstrates that the heterogeneous reaction is controlling the process. This explains the findings where the mass rate of ARTOK varied with

temperature due to chemical kinetic control, while AROK did not exhibit significant variation with temperature. AROK did not exhibit significant variation because there was a higher resistance to oxygen reaching the particle surface for char oxidation, even as the temperature was increased. The temperature dependence is high when chemical reaction is the rate-controlling step and low if the mass transfer is rate-controlling [67].

Based on the recorded values during the batch pyrolysis experiment at  $T = 550$  °C (see Fig. 12), the char yield was found to be 21.5% for AROK and 24% for ARTOK. The torrefied biomass formed more biochar in pyrolysis [66]. Putting the mass feed rate (from Table 2) at ER = 0.2 for AROK and ARTOK into Eq. 7 allowed the values of char feed rate (F) to be calculated.

The values of steady state mass for AROK and ARTOK were obtained with a MATLAB program using linear change point models based on Eq. (16) [68]. This equation shows the relationship between mass and time.

$$Y = \beta_1 + \beta_2(X - \beta_3)^+ \quad (16)$$

where  $\beta_1$  is steady state mass,  $\beta_2$  is the slope,  $\beta_3$  is critical point time,  $X$  is the input time,  $(^+)$  means that only positive differences between  $X$  and  $\beta_3$  are taken into account, and  $Y$  is the output mass.

The rate constant  $k$  was evaluated experimentally at steady state char loading in the reactor using Eq. (13). The values of  $F$  and  $k$  are substituted into Eq. (12) yielding the mass balance model for the char load in the reactor. The predicted behaviour of AROK and ARTOK is shown in Fig. 11 together with the corresponding experimental data at different temperatures. It can be seen that this model is also a good fit to the experimental data. ARTOK exhibits higher regression than AROK (between 95 and 99%), which means ARTOK obeys a first order reaction model more so than AROK. The calculated value of  $k$  for different steady state reaction temperatures (see Fig. 3) using the results of Fig. 11 are included in Table 3;  $m_{ss}$  denotes the steady state condition mass of char in the reactor.

From the results presented in Table 3 the Arrhenius equation can be plotted for  $k$  in terms of reciprocal temperature. Linear regression of the data in Fig. 13 yields the best fit line shown. From the  $\ln(k)$  versus  $1/T$  plot, the slope ( $E_a/R$ ) was used to obtain the values of activation energies for the AROK and ARTOK, giving activation energies of 84 and 106 kJ/mol respectively. This means that a lower amount of energy is necessary for the raw olive kernel to start reacting than for torrefied biomass [69].

At present, there is limited information available in the literature that focuses on the gasification kinetics of raw and torrefied biomass. However, the activation energy of seed corn biomass was found to be 78 kJ/mol during gasification in a bubbling fluidised bed during continuous gasification

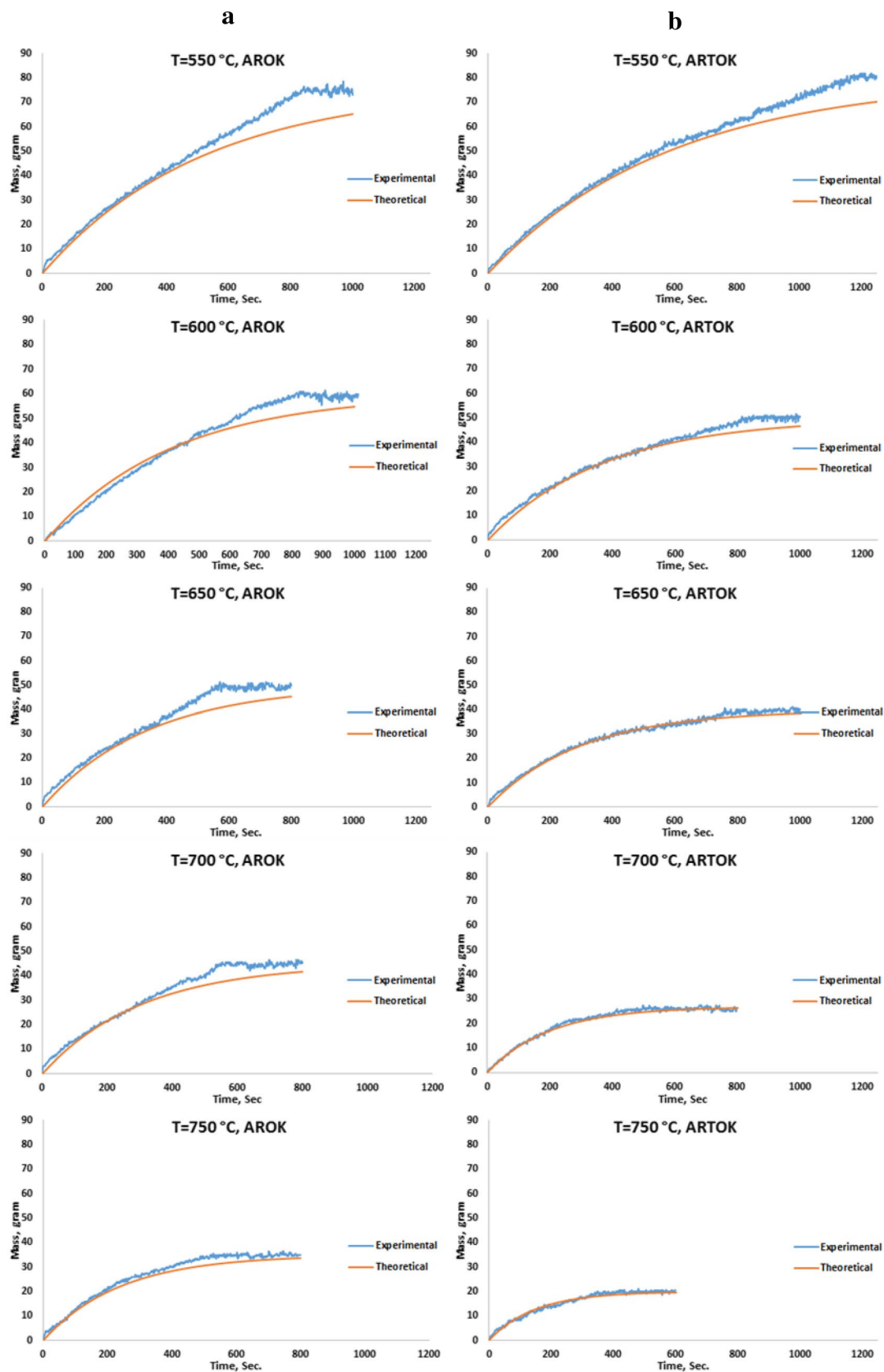


**Fig. 11** Calculated mass of the char of in the gasifier as measured by experimental work and predicated by the mass balance model at different preset temperatures for **a** AROK and **b** ARTOK

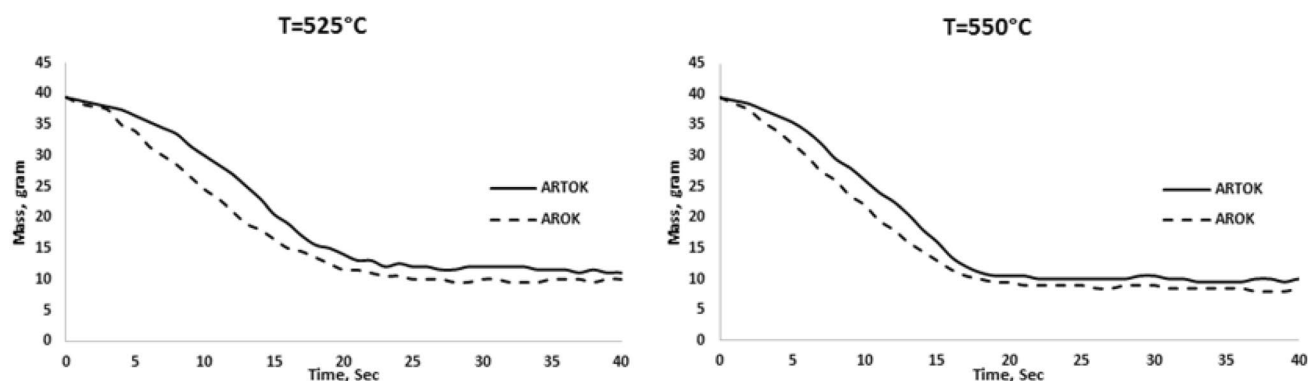


**Fig. 12** Mass loss with time of AROK and ARTOK under pyrolysis conditions at temperature 525 and 550 °C

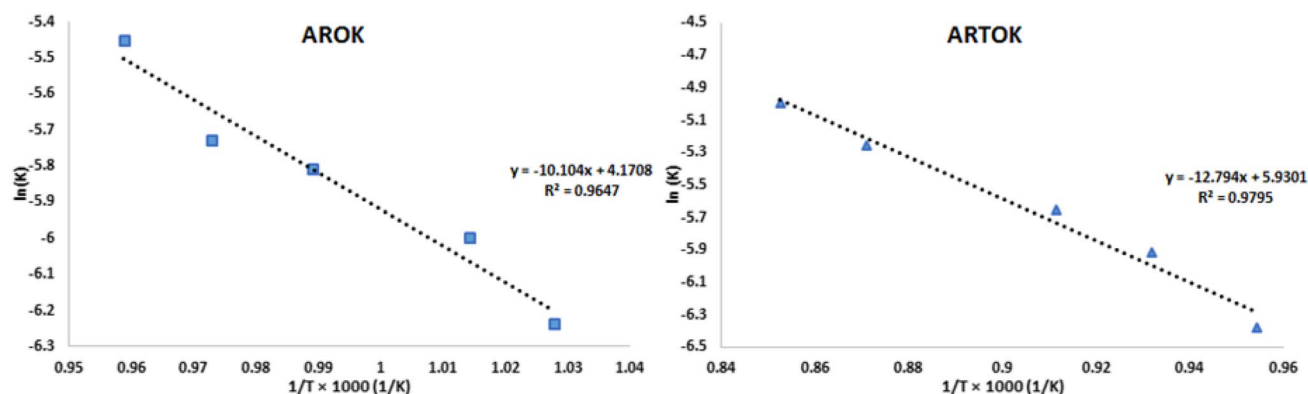


**Fig. 13** Arrhenius plot for AROK and ARTOK

by using a transient model, and it was suggested that the reactions are limited by pore diffusion, therefore this value represented the apparent activation energy [30]. In many gas–solid systems with comparatively fast reactions, the overall rate is found to be controlled by mass transport between the reaction surface and the bulk fluid [59]. According to the same author, in the experimental determination of kinetic parameters, it is very important to ensure that the measurements are carried out under conditions such that the overall rate is indeed controlled by chemical kinetics, where pore diffusion and gas phase mass transfer do not play a significant role. The activation energy of ARTOK measured here suggests that the reactions are chemical reaction controlled compared with AROK. However, the activation energy of raw olive kernel under inert conditions (pyrolysis) has been investigated in previous work and found equal to 60.8 kJ/mol; less than the activation energy of gasification of AROK [14], which agreed well with results of others [70, 71], who found the activation energy in air was higher than in a nitrogen atmosphere.

## Conclusions

Raw and torrefied olive kernels were gasified in a thermogravimetric bubbling fluidised bed gasifier to investigate the influence of temperature and ER on the gasification performance. Such experimental results gave considerable information about performance and potential scaling-up in order to explore the possible benefits of ARTOK over AROK. The use of torrefaction can be expanded if the product gas quality as well as cold gas efficiency are improved through gasification of pre-treated biomass. On the basis of the data obtained for the gasification in the studied range of operating process parameters the following conclusions are made:

- The raw and torrefied biomass showed different characteristics, resulting in different gas composition and heating value. Torrefied biomass showed consistently higher product gas heating value and cold gas efficiency, which was attributed to higher production rates of CO, H<sub>2</sub> and light hydrocarbons.

- The first order reaction model was found to be appropriate for both types of biomass (AROK and ARTOK) thus providing a reasonable description of the biomass reaction.
- The reaction characteristics of raw and torrefied biomass in oxidative atmospheres at various temperatures have been investigated and qualitative agreement between model prediction and experimental data was achieved. From the kinetic analysis carried out, the results suggest that the reaction was controlled by mass transfer in the parent sample, while char oxidation was the controlling factor in the torrefied sample.
- External diffusion has the minimize test affect at high superficial velocity.
- By comparing experimental results, thermal pre-treatment of biomass before gasification is a promising concept for the operation of full-scale processes.
- The kinetics of biomass gasification continues to be a subject of concentrated investigation. However, the results of such investigations to date, have only flowed into the design procedures for commercial gasification reactors to a limited extent. The suppressed external diffusion limitations and higher heating rate prevailing in the TGFBR were responsible for all these kinetic parameters. They demonstrate the capability and superiority of the TGFBR for analysing biomass gasification, and it is believed that this data provides a deep insight into the gasification mechanism, and gasifier design, which could help with future commercial reactors.

**Acknowledgements** We express our sincere thanks to the Iraqi Ministry of Higher Education/AL-Nahrain University for their financial support under Contract Number 6052.

**Open Access** This article is distributed under the terms of the Creative Commons Attribution 4.0 International License (<http://creativecommons.org/licenses/by/4.0/>), which permits unrestricted use, distribution, and reproduction in any medium, provided you give appropriate credit to the original author(s) and the source, provide a link to the Creative Commons license, and indicate if changes were made.

## References

1. Sadaka, S.S.: Gasification of raw and torrefied cotton gin wastes in an auger system. *Appl. Eng. Agric.* **29**(3), 405–414 (2013)
2. Gai, C., Dong, Y., Lv, Z., Zhang, Z., Liang, J., Liu, Y.: Pyrolysis behavior and kinetic study of phenol as tar model compound in micro fluidized bed reactor. *Int. J. Hydrogen Energy*. **40**, 7956–7964 (2015)
3. Esfahani, R.M., Wan Ab Karim Ghani, W.A., Mohd Salleh, M.A., Ali, S.: Hydrogen-rich gas production from palm kernel shell by applying air gasification in fluidized bed reactor. *Energy Fuels*. **26**, 1185–1191 (2012)
4. van der Stelt, M.J.C., Gerhauser, H., Kiel, J.H.A., Ptasiński, K.J.: Biomass upgrading by torrefaction for the production of biofuels: a review. *Biomass Bioenerg.* **35**, 3748–3762 (2011)
5. Dudyński, M., van Dyk, J.C., Kwiatkowski, K., Sosnowska, M.: Biomass gasification: influence of torrefaction on syngas production and tar formation. *Fuel Process. Technol.* **131**, 203–212 (2015)
6. Gómez-Barea, A., Leckner, B.: Modeling of biomass gasification in fluidized bed. *Prog. Energy Combust. Sci.* **36**, 444–509 (2010)
7. Reschmeier, R., Roveda, D., Müller, D., Karl, J.: Pyrolysis kinetics of wood pellets in fluidized beds. *J. Anal. Appl. Pyrol.* **108**, 117–129 (2014)
8. López-González, D., Fernandez-Lopez, M., Valverde, J.L., Sanchez-Silva, L.: Gasification of lignocellulosic biomass char obtained from pyrolysis: kinetic and evolved gas analyses. *Energy*. **71**, 456–467 (2014)
9. Ollero, P., Serrera, A., Arjona, R., Alcantarilla, S.: Diffusional effects in TGA gasification experiments for kinetic determination. *Fuel*. **81**, 1989–2000 (2002)
10. Khalil, R., Várhegyi, G., Jäschke, S., Grønli, M.G., Hustad, J.: CO<sub>2</sub> gasification of biomass chars: a kinetic study. *Energy Fuels*. **23**, 94–100 (2008)
11. Xue, G., Kwapinska, M., Kwapinski, W., Czajka, K.M., Kennedy, J., Leahy, J.J.: Impact of torrefaction on properties of *Miscanthus × giganteus* relevant to gasification. *Fuel*. **121**, 189–197 (2014)
12. Jian, Y.U., Zhu, J.H., Feng, G.U.O., Duan, Z.K., Liu, Y.Y., Xu, G.W.: Reaction kinetics and mechanism of biomass pyrolysis in a micro-fluidized bed reactor. *J. Fuel Chem. Technol.* **38**, 666–672 (2010)
13. Miura, K., Silveston, P.L.: Analysis of gas-solid reactions by use of a temperature-programmed reaction technique. *Energy Fuels*. **3**, 243–249 (1989)
14. Al-Farraj, A., Marsh, R., Steer, J.: A Comparison of the pyrolysis of olive kernel biomass in fluidised and fixed bed conditions. *Waste Biomass Valoriz.* **8**, 1–12 (2017)
15. Lahijani, P., Zainal, Z.A.: Gasification of palm empty fruit bunch in a bubbling fluidized bed: a performance and agglomeration study. *Biores. Technol.* **102**, 2068–2076 (2011)
16. Song, T., Wu, J., Shen, L., Xiao, J.: Experimental investigation on hydrogen production from biomass gasification in interconnected fluidized beds. *Biomass Bioenerg.* **36**, 258–267 (2012)
17. Phanphanich, M., Mani, S.: Impact of torrefaction on the grindability and fuel characteristics of forest biomass. *Biores. Technol.* **102**, 1246–1253 (2011)
18. Bergman, P.C., Boersma, A., Zwart, R., Kiel, J.: Torrefaction for biomass co-firing in existing coal-fired power stations. Energy Centre of Netherlands, Report No. ECN-C-05–013 (2005)
19. Poudel, J., Oh, S.C.: Effect of torrefaction on the properties of corn stalk to enhance solid fuel qualities. *Energies*. **7**, 5586–5600 (2014)
20. Gauthier, D., Zerguerras, S., Flamant, G.: Influence of the particle size distribution of powders on the velocities of minimum and complete fluidization. *Chem. Eng. J.* **74**, 181–196 (1999)
21. Choi, J.-H., Suh, J.-M., Chang, I.-Y., Shun, D.-W., Yi, C.-K., J.-Son, E., et al.: The effect of fine particles on elutriation of coarse particles in a gas fluidized bed. *Powder Technol.* **121**, 190–194 (2001)
22. Kunii, D., Levenspiel, O.: Fluidization engineering. Elsevier, Amsterdam (2013)
23. Li, X.T., Grace, J.R., Lim, C.J., Watkinson, A.P., Chen, H.P., Kim, J.R.: Biomass gasification in a circulating fluidized bed. *Biomass Bioenerg.* **26**, 171–193 (2004)



24. Xiao, R., Zhang, M., Jin, B., Huang, Y., Zhou, H.: High-temperature air/steam-blown gasification of coal in a pressurized spout-fluid bed. *Energy Fuels*. **20**, 715–720 (2006)
25. Natarajan, E., Nordin, A., Rao, A.N.: Overview of combustion and gasification of rice husk in fluidized bed reactors. *Biomass Bioenerg.* **14**, 533–546 (1998)
26. Demirbas, A.: Effects of temperature and particle size on bio-char yield from pyrolysis of agricultural residues. *J. Anal. Appl. Pyrol.* **72**, 243–248 (2004)
27. Bates, R.B., Altantzis, C., Ghoniem, A.F.: Modeling of biomass char gasification, combustion, and attrition kinetics in fluidized beds. *Energy Fuels*. **30**, 360–376 (2016)
28. Zabaniotou, A.A., Kalogiannis, G., Kappas, E., Karabelas, A.J.: Olive residues (cuttings and kernels) rapid pyrolysis product yields and kinetics. *Biomass Bioenerg.* **18**, 411–420 (2000)
29. Di Blasi, C.: Kinetic and heat transfer control in the slow and flash pyrolysis of solids. *Ind. Eng. Chem. Res.* **35**, 37–46 (1996)
30. Timmer, K.J.: Carbon conversion during bubbling fluidized bed gasification of biomass: ProQuest, Ann Arbor (2008)
31. Scala, F., Salatino, P., Chirone, R.: Fluidized bed combustion of a biomass char (*Robinia pseudoacacia*). *Energy Fuels*. **14**, 781–790 (2000)
32. Chang, A.C.C., Chang, H.-F., Lin, F.-J., Lin, K.-H., Chen, C.-H.: Biomass gasification for hydrogen production. *Int. J. Hydrogen Energy*. **36**, 14252–14260 (2011)
33. House, J.E.: Principles of Chemical Kinetics 2nd edn. Elsevier, Amsterdam (2007)
34. Van de Velden, M., Baeyens, J., Brems, A., Janssens, B., Dewil, R.: Fundamentals, kinetics and endothermicity of the biomass pyrolysis reaction. *Renew. Energy*. **35**, 232–242 (2010)
35. Saddawi, A., Jones, J., Williams, A., Wojtowicz, M.: Kinetics of the thermal decomposition of biomass. *Energy Fuels*. **24**, 1274–1282 (2009)
36. Caballero, J.A., Font, R., Marcilla, A., Conesa, J.A.: New kinetic model for thermal decomposition of heterogeneous materials. *Ind. Eng. Chem. Res.* **34**, 806–812 (1995)
37. Bridgeman, T.G., Jones, J.M., Shield, I., Williams, P.T.: Torrefaction of reed canary grass, wheat straw and willow to enhance solid fuel qualities and combustion properties. *Fuel*. **87**, 844–856 (2008)
38. Ibrahim, R.H., Darvell, L.I., Jones, J.M., Williams, A.: Physico-chemical characterisation of torrefied biomass. *J. Anal. Appl. Pyrol.* **103**, 21–30 (2013)
39. Prins, M.J., Ptasiński, K.J., Janssen, F.J.J.G.: More efficient biomass gasification via torrefaction. *Energy*. **31**, 3458–3470 (2006)
40. Basu, P.: Biomass gasification and pyrolysis: practical design and theory. Academic press, Cambridge (2010)
41. Chen, W.-H., Chen, C.-J., Hung, C.-I., Shen, C.-H., Hsu, H.-W.: A comparison of gasification phenomena among raw biomass, torrefied biomass and coal in an entrained-flow reactor. *Appl. Energy*. **112**, 421–430 (2013)
42. Cao, Y., Wang, Y., Riley, J.T., Pan, W.-P.: A novel biomass air gasification process for producing tar-free higher heating value fuel gas. *Fuel Process. Technol.* **87**, 343–353 (2006)
43. Skoulou, V., Koufodimos, G., Samaras, Z., Zabaniotou, A.: Low temperature gasification of olive kernels in a 5-kW fluidized bed reactor for H<sub>2</sub>-rich producer gas. *Int. J. Hydrogen Energy*. **33**, 6515–6524 (2008)
44. Mohammed, M.A.A., Salmiaton, A., Wan Azlina, W.A.K.G., Mohammad Amran, M.S., Fakhru'l-Razi A.: Air gasification of empty fruit bunch for hydrogen-rich gas production in a fluidized-bed reactor. *Energy Convers. Manag.* **52**, 1555–1561 (2011)
45. Lucas, C., Szewczyk, D., Blasiak, W., Mochida, S.: High-temperature air and steam gasification of densified biofuels. *Biomass Bioenerg.* **27**, 563–575 (2004)
46. Abdoulmoumine, N., Kulkarni, A., Adhikari, S.: Effects of temperature and equivalence ratio on pine syngas primary gases and contaminants in a bench-scale fluidized bed gasifier. *Ind. Eng. Chem. Res.* **53**, 5767–5777 (2014)
47. Xue, G., Kwapinska, M., Horvat, A., Kwapinski, W., Rabou, L., Dooley, S., et al.: Gasification of torrefied *Miscanthus × giganteus* in an air-blown bubbling fluidized bed gasifier. *Bioresour. Technol.* **159**, 397–403 (2014)
48. Kuo, P.-C., Wu, W., Chen, W.-H.: Gasification performances of raw and torrefied biomass in a downdraft fixed bed gasifier using thermodynamic analysis. *Fuel*. **117**(Part B), 1231–1241 (2014)
49. Couhert, C., Salvador, S., Commandré, J.M.: Impact of torrefaction on syngas production from wood. *Fuel*. **88**, 2286–2290 (2009)
50. Kwapinska, M., Xue, G., Horvat, A., Rabou, L.P., Dooley, S., Kwapinski, W., et al.: Fluidized bed gasification of torrefied and raw grassy biomass (*Miscanthus × giganteus*). The effect of operating conditions on process performance. *Energy Fuels*. **29**, 7290–7300 (2015)
51. Emami Taba, L., Irfan, M.F., Wan Daud, W.A.M., Chakrabarti, M.H.: The effect of temperature on various parameters in coal, biomass and CO-gasification: a review. *Renew. Sustain. Energy Rev.* **16**, 5584–5596 (2012)
52. Gil, J., Corella, J., Aznar, M.A.P., Caballero, M.A.: Biomass gasification in atmospheric and bubbling fluidized bed: effect of the type of gasifying agent on the product distribution. *Biomass Bioenerg.* **17**, 389–403 (1999)
53. Loha, C., Chattopadhyay, H., Chatterjee, P.K.: Three dimensional kinetic modeling of fluidized bed biomass gasification. *Chem. Eng. Sci.* **109**, 53–64 (2014)
54. Narvaez, I., Orio, A., Aznar, M.P., Corella, J.: Biomass gasification with air in an atmospheric bubbling fluidized bed. Effect of six operational variables on the quality of the produced raw gas. *Ind. Eng. Chem. Res.* **35**, 2110–2120 (1996)
55. Ahmad, A.A., Zawawi, N.A., Kasim, F.H., Inayat, A., Khasri, A.: Assessing the gasification performance of biomass: a review on biomass gasification process conditions, optimization and economic evaluation. *Renew. Sustain. Energy Rev.* **53**, 1333–1347 (2016)
56. Dhungana, A.: Torrefaction of biomass. *Can. J. Chem. Eng.* **90**(1), 186–195 (2011)
57. Chen, Q., Zhou, J., Liu, B., Mei, Q., Luo, Z.: Influence of torrefaction pretreatment on biomass gasification technology. *Chin. Sci. Bull.* **56**, 1449–1456 (2011)
58. Klawekla, R., Arend, M., Hoelderich, W.F.: A review of mass transfer controlling the reaction rate in heterogeneous catalytic systems, vol. 5. INTECH Open Access Publisher, Rijeka (2011)
59. Szekely J., Sohn H.Y., Gas-Solid Reactions. Academic Press, Cambridge (1976)
60. Fogler, H.S.: Elements of chemical reaction engineering, 4th edn. p. 1. Pearson Education Limited, Edinburgh (2014)
61. Wang, F., Zeng, X., Shao, R., Wang, Y., Yu, J., Xu, G.: Isothermal gasification of in situ/ex situ coal char with CO<sub>2</sub> in a micro fluidized bed reaction analyzer. *Energy Fuels*. **29**, 4795–4802 (2015)
62. Guo, F., Dong, Y., Lv, Z., Fan, P., Yang, S., Dong, L.: Kinetic behavior of biomass under oxidative atmosphere using a micro-fluidized bed reactor. *Energy Convers. Manag.* **108**, 210–218 (2016)
63. Sami, M., Annamalai, K., Wooldridge, M.: Co-firing of coal and biomass fuel blends. *Prog. Energy Combust. Sci.* **27**, 171–214 (2001)
64. Hu, W., Yang, X., Mi, B., Liang, F., Zhang, T., Fei, B., et al.: Investigating chemical properties and combustion characteristics of torrefied masson pine. *Wood Fiber Sci.* **49**, 33–42 (2017)
65. Protásio, T.D.P., Melo, I.C.N.A.D., Guimarães, M. Jr., Mendes, R.F., Trugilho, P.F.: Thermal decomposition of torrefied and

- carbonized briquettes of residues from coffee grain processing. *Ciência e Agrotecnol.* **37**, 221–228 (2013)
66. Ren, S., Lei, H., Wang, L., Bu, Q., Chen, S., Wu, J.: Thermal behaviour and kinetic study for woody biomass torrefaction and torrefied biomass pyrolysis by TGA. *Biosyst. Eng.* **116**, 420–426 (2013)
67. Latif, A.: A study of the design of fluidized bed reactors for biomass gasification. University of London, London (1999)
68. Zhang, Y., O'Neill, Z., Dong, B., Augenbroe, G.: Comparisons of inverse modeling approaches for predicting building energy performance. *Build. Environ.* **86**, 177–190 (2015)
69. Uhrig, A., Determination of pyrolysis reaction kinetics of raw and torrefied biomass. Bachelor's thesis, University of Twente (2014)
70. Sait, H.H., Hussain, A., Salema, A.A., Ani, F.N.: Pyrolysis and combustion kinetics of date palm biomass using thermogravimetric analysis. *Biores. Technol.* **118**, 382–389 (2012)
71. Munir, S., Daood, S.S., Nimmo, W., Cunliffe, A.M., Gibbs, B.M.: Thermal analysis and devolatilization kinetics of cotton stalk, sugar cane bagasse and shea meal under nitrogen and air atmospheres. *Biores. Technol.* **100**, 1413–1418 (2009)